Compatibility at Polymer/Polymer Mixture Interfaces in the Presence of Solvent

Kyung-Sup Yoon, Hyungsuk Pak*, Jo Woong Lee, and Taihyun Chang†

Department of Chemistry, Seoul National University, Seoul 151-742
†Department of Chemistry, Pohang Institute of Science and Technology, Pohang 790-600
Received October 13, 1993

We present some results obtained from theoretical study on a non-symmetrical A/BC polymeric system including solvent which consists of two phases, a polymeric phase A on one side and a mixture of polymers B (as a compatibilizer) and C on the other in the presence of a solvent. By employing the functional integral techniques we derive the mean-field equations and solve them numerically to deduce the physical properties of the interface involving the polymers and solvent concentration profiles in the limit that molecular weights of all the polymers involved tend to infinity. The calculations are performed for typical values of the Flory interaction parameters and for the volume fraction of polymer B in the asymptotic phase and of solvent. In the polymers/solvent blend under consideration the interfacial adsorption of polymer B, the solvent concentration, and degrees of the specific interaction between the polymers are found to play important roles in modification of the interfacial properties.

Introduction

A great deal of interest has thus far been focused on experimental[1-5] and theoretical[6-21] studies of the interfacial properties in heterogeneous multicomponent polymeric systems. Helfand and co-workers[8-10] have developed a theory, based on mean-field ideas, for predicting the interfacial properties of the polymer/polymer systems. Noolandi and co-workers[13,14,16] have also presented fully self-consistent calculations of the polymer concentration profile and consequent interfacial tension at polymer/polymer interfaces in the presence of a solvent and/or block copolymers. However, relatively little work has been done to extend these results to the immiscible polymer/polymer system including third homopolymers as compatibilizers,[3b] the presence of which may be expected to improve the interfacial adhesion between the immiscible polymers by slowing the phase demixing process in the blends and to usually result in the intrinsic non-symmetrical interfaces.

Recently Helfand[17] has extended the theory of the A/B polymeric interface[8,10] to the specific case of the interfacial tension in the A/BC polymeric interface *via* equations of motion.[8-10,19b,22] By employing the functional integral methods[13,23-25] Yoon and Pak[6] have also published the results of the interfacial properties including the concentration profiles for two-phase interface in the A/BC system, which is the same model as adopted by Helfand,[17] where two phases consist of a polymeric phase A on one side and a mixture of polymers B and C on the other.

In this paper we describe a method of extending this approach to take into account the effect of solvent additionally present in the A/BC system. The mean-field equations are derived in the limit of a vanishingly small compressibility and infinitely large molecular weights for all the polymers involved and solved numerically by a self-consistent procedure in the presence of a solvent. We will assume that the interface between two phases is planar. However, there seems to be no sharply defined boundary in the actual interfacial region, therefore, it is convenient to choose the mathematical dividing surface as an interface, which will be taken as the Gibbs dividing surface[17,26] for polymer A. The calculations of interfacial properties are performed for typical values of the Flory interaction parameters,[27,28] χ_{AC} and χ_{BC} (as negative value), the volume fraction of polymer B in the asymptotic mixture phase, $\phi_B(\infty)$, and that of solvent, ϕ_S^0. As the results, we obtain the concentration profiles, the interfacial tension, the amount of polymer B adsorbed to the interface, the widths of solvent and total interface, and the overlap lengths between the polymers. The interfacial adsorption of polymer B, the solvent concentration, and degrees of the specific interaction between the polymers play an important role in modification of the interfacial properties.

The following sections contain the general theory for the polymers/solvent systems based on the mean-field approximation, the case of infinite molecular weight for the polymers as a good approximation, the numerical method used to solve the mean-field equations, and the results of the calculation of the physical properties of the interface. In the end we remark the conclusions.

Theory

Partition Function. The polymer chains will be looked upon as space curves with τ varying from 0 to Z_P, the degree of polymerization. Hereafter, we use the letter K to symbolize the polymer of type $P(P=A, B,$ or $C)$ or solvent (S). The space curves $\{\boldsymbol{r}_P(\cdot)\}$, which represent possible configurations of the polymers and are Gaussianly distributed, are continuous with the rate of extension at each point $d\boldsymbol{r}_P/d\tau$. The probability density functional for a given space curve is

$$P[\{\boldsymbol{r}_P(\cdot)\}] \propto \exp\left\{-\frac{3}{2b_P^2}\int_0^{Z_P} d\tau\left[\frac{d\boldsymbol{r}_P(\tau)}{d\tau}\right]^2\right\} \quad (1)$$

where b_P is the Kuhn statistical length.[8,11]

Assuming the polymers/solvent blend under consideration to be incompressible, the partition function is given as a functional integral of the probability density functional with

the incompressibility constraint over all possible configurations in the field of intermolecular potential, $\hat{W}[\{r_{Ki}(\cdot)\}]$, in units of k_BT, viz.

$$Z=\left(\prod_K \frac{Z_K^{\tilde{N}_K}}{\tilde{N}_K!}\right)\int \prod_K \prod_i^{\tilde{N}_K} d[\{r_{Ki}(\cdot)\}]P[\{r_{Ki}(\cdot)\}] \times \delta\left[1-\sum_K \frac{\hat{\rho}_K(\cdot)}{\rho_{0K}}\right] \exp\{\hat{W}[\{r_{Ki}(\cdot)\}]\} \quad (2)$$

Here Z_K is the contribution to the partition function from the kinetic energy. $\tilde{N}_K=N_K/Z_K$ is the number of molecules, N_P is the total number of monomer units for polymer P, N_S is the number of solvent molecules, and since $Z_S=1$, $\tilde{N}_S=N_S$. The delta function ensures an incompressibility, and ρ_{0K} is the density of pure compouent K in monomer segments per unit volume.

As described in Ref. (6), the partition function can be written as

$$Z=\mathrm{No}\int\left[\prod_K d\rho_K(\cdot)d\omega_K(\cdot)\right]d\eta(\cdot) \times \exp\{-F_T[\{\rho_K(\cdot)\},\{\omega_K(\cdot)\},\eta(\cdot)]\} \quad (3)$$

where No is a normalization constant, and F_T, the total free energy functional in units of k_BT, is given by

$$F_T[\{\rho_K(\cdot)\},\{\omega_K(\cdot)\},\eta(\cdot)]=\frac{1}{2}\sum_K \rho_{0K}W_{KK}N_K+\frac{1}{2}\sum_{KK'}\int d\boldsymbol{r}\rho_K(\boldsymbol{r})U_{KK'}\rho_{K'}(\boldsymbol{r}) -\sum_K\int d\boldsymbol{r}\omega_K(\boldsymbol{r})\rho_K(\boldsymbol{r})+\sum_K \tilde{N}_K\left[\ln\left(\frac{\tilde{N}_K}{Z_K J_K}\right)-1\right] +\int d\boldsymbol{r}\eta(\boldsymbol{r})\left[\sum_K \frac{\rho_K(\boldsymbol{r})}{\rho_{0K}}-1\right] \quad (4)$$

Here $W_{KK}=\int d\boldsymbol{r}W_{KK}(\boldsymbol{r})$, $U_{KK'}=\int d\boldsymbol{r}U_{KK'}(\boldsymbol{r})$ [the potential energy, $U_{KK'}(\boldsymbol{r})$, vanishes for the interactions between like molecules.], $\omega_K(\boldsymbol{r})$ is the mean field acting on the polymer, and the field $\eta(\boldsymbol{r})$ is the Lagrangian multiplier corresponding to the constraint of no volume change locally upon mixing. In the intermolecular potential the gradient terms that may be generally negligible[10,14b] are excluded, and

$$N_K=\int d\boldsymbol{r}\rho_K(\boldsymbol{r}) \quad (5)$$

When the system is uniform all over, from Eq. (4) the local homogeneous free energy density in units of k_BT is given in terms of the chemical potential of pure components by

$$f_h=\sum_K \mu_{0K}\rho_K(\boldsymbol{r})+\frac{1}{2}\sum_{KK'}\rho_K(\boldsymbol{r})U_{KK'}\rho_{K'}(\boldsymbol{r})+\sum_K \frac{\rho_K(\boldsymbol{r})}{Z_K}\ln\left(\frac{\rho_K(\boldsymbol{r})}{\rho_{0K}}\right) \quad (6)$$

In Eq. (4) the quantities J_P can be expressed in terms of the distribution function, $Q_P(\boldsymbol{r},\tau|\boldsymbol{r}_0)$ for a chain of τ repeat units to start at $\boldsymbol{r}_0$ and end at $\boldsymbol{r}$, which can be interpreted as the propagator of the inhomogeneous differential equation.[9,13,25] The following function $q_P(\boldsymbol{r},\tau)$ can be expressed as the integrals of $Q_P(\boldsymbol{r},\tau|\boldsymbol{r}_0)$ over all the starting positions $\boldsymbol{r}_0$, and then the function $q_P(\boldsymbol{r},\tau)$ can be solved from the modified diffusion equation, viz.

$$\left[\frac{1}{Z_P}\frac{\partial}{\partial\tau}-\frac{b_P^2}{6}\nabla^2+\omega_P(\boldsymbol{r})\right]q_P(\boldsymbol{r},\tau)=\delta(\tau) \quad (7)$$

In polymer chains with the length Z_P, any segment of length $Z_P\tau$ may be regarded as the origin of two walks, one of length $Z_P\tau$ and one of length $Z_P(1-\tau)$. Thus $q_P(\boldsymbol{r},Z_P)$ can be written as two distribution functions, *i.e.*, one is $q_P(\boldsymbol{r},Z_P\tau)$, and the other $q_P[\boldsymbol{r},Z_P(1-\tau)]$:

$$J_P=\int d\boldsymbol{r}q_P(\boldsymbol{r},Z_P)=\int d\boldsymbol{r}q_P(\boldsymbol{r},Z_P,\tau)q_P[\boldsymbol{r},Z_P(1-\tau)] \quad (8)$$

Mean-Field Approximation. Using the saddle-function technique,[9,13] we obtain the mean-field equations, given by minimization of the free energy functional, Eq. (4), with respect to each $\omega_K(\boldsymbol{r})$, $\rho_K(\boldsymbol{r})$ and $\eta(\boldsymbol{r})$, subject to the constraint of the constant number of monomers, Eq. (5). The minimization equation for $\omega_K(\boldsymbol{r})$ is given by

$$\rho_P(\boldsymbol{r})=\frac{N_P}{J_P}\int_0^1 d\tau q_P(\boldsymbol{r},\tau)q_P(\boldsymbol{r},1-\tau)$$
$$\rho_S(\boldsymbol{r})=\frac{N_S}{J_S}\exp[-\omega_S(\boldsymbol{r})] \quad (9)$$

where J_K satisfies the relation $N_K/J_K=\rho_{0K}$.[13,14] From Eqs. (4), (6), and (9) the free energy, F, is written as follows

$$F=\int d\boldsymbol{r}\left\{f_h-\sum_P \rho_P(\boldsymbol{r})\left[\omega_P(\boldsymbol{r})+\frac{1}{Z_P}\ln\left(\frac{\rho_P(\boldsymbol{r})J_P}{N_P}\right)\right]\right\} \quad (10)$$

Then the minimization for $\rho_K(\boldsymbol{r})$ yields the following equation:

$$\frac{\partial f_h}{\partial\rho_K(\boldsymbol{r})}-\left[\omega_P(\boldsymbol{r})+\frac{1}{Z_P}\ln\left(\frac{\rho_P(\boldsymbol{r})}{\rho_{0P}}\right)\right]+\frac{\eta(\boldsymbol{r})}{\rho_{0K}}-\lambda_K=0 \quad (11)$$

where λ_K is the Lagrangian multiplier associated with the constraint of the constant number of monomers, Eq. (5), and the first term in the above equation is the chemical potential of component K. Using the relations for solvent and the asymptotic phases, the polymer mean field in Eq. (11) is given by

$$\omega_P(\boldsymbol{r})=\frac{\partial\Delta f}{\partial\rho_P(\boldsymbol{r})}-\frac{1}{Z_P}\ln\left(\frac{\rho_P(\boldsymbol{r})}{\rho_{0P}}\right)-\frac{\rho_{0S}}{\rho_{0P}}\frac{\partial\Delta f}{\partial\rho_S(\boldsymbol{r})} \quad (12)$$

The minimization equation for $\eta(\boldsymbol{r})$ is

$$\sum_K \frac{\rho_K(\boldsymbol{r})}{\rho_{0K}}=1 \quad (13)$$

which makes the last term in Eq. (4) zero at the saddle-point.

The local homogeneous free energy density relative to the asymptotic phases using Eq. (6) can be written as

$$\Delta f/\rho_0=\sum_K \frac{\rho_{0K}}{\rho_0}\phi_K(\boldsymbol{r})(\mu_{0K}-\mu_K{}^b)+\frac{1}{2}\sum_{KK'}\chi_{KK'}\phi_K(\boldsymbol{r})\phi_{K'}(\boldsymbol{r}) +\sum_K \frac{\rho_{0K}}{\rho_0}\frac{\phi_K(\boldsymbol{r})}{Z_K}\ln\phi_K(\boldsymbol{r}) \quad (14)$$

where ρ_0 is the reference density, the volume fraction $\phi_K(\boldsymbol{r})$ is defined by $\phi_K(\boldsymbol{r})=\hat{\rho}_K(\boldsymbol{r})/\sum\hat{\rho}_K(\boldsymbol{r})$ with the reduced density which defined by $\hat{\rho}_K(\boldsymbol{r})=\rho_K(\boldsymbol{r})/\rho_{0K}$, and $\chi_{KK'}=U_{KK'}\rho_{0K}\rho_{0K'}/\rho_0$ is the usual Flory interaction parameter with k_BT as the unit of energy.

The interfacial tension can be obtained from the equation

$$F=\gamma A+\sum_K N_K\mu_K{}^b \quad (15)$$

where A is the interfacial area. Then the interfacial tension, in units of k_BT, can be rewritten in terms of the free energy

density relative to the asymptotic bulk phases, the conformational entropy, and the combinatorial entropy which has relation with the degree of polymerization

$$\gamma A/\rho_0=\int dr\Big\{\Delta f/\rho_0-\sum_P \frac{\rho_{0P}}{\rho_0}\int_0^1 d\tau\,\frac{b_P^2}{6}\nabla^2 q_P(r,\tau)q_P(r,1-\tau)\Big\}$$
$$+\int dr\Big\{\sum_P \frac{\rho_{0P}}{\rho_0}\frac{1}{Z_P}\Big[\int_0^1 d\tau\frac{\partial q_P(r,\tau)}{\partial\tau}q_P(r,1-\tau)-\phi_P(r)\ln\phi_P(r)\Big]\Big\} \quad (16)$$

Infinite Molecular Weight

For most polymeric systems the physical properties, in reality, depend on the degree of polymerization.[3,15,19] In here we assume the infinite molecular weight for the polymers as a good approximation. For simplicity, we take $\rho_{0K}=\rho_0$, $b_P=b$ for all components and consider the one-dimensional nature for the interfacial problem. With these assumptions,[8,10,11] the solution of Eq. (7) for $\tau>0$ may be written in the separable form, $q_P(x,\tau)=[\phi_P(\pm\infty)]^\tau Q_P(x)$ where $q_P(x,\tau)$ satisfies the boundary condition, $q_P(\pm\infty,\tau)=[\phi_P(\pm\infty)]^\tau$, when $|x|\to\infty$ in Eq. (7), and $Q_P(x)$ satisfies the following equation:

$$\frac{b^2}{6}\frac{d^2Q_P}{dx^2}-\omega_P(x)Q_P=0 \quad (17)$$

The polymer volume fraction is then given by

$$\phi_P(x)=\phi_P(\pm\infty)[Q_P(x)]^2 \quad (18)$$

Centering aground the interface, $x=0$, which is selected as the Gibbs dividing surface for polymer A, the negative x region is polymer A rich, and the positive one is polymers B and C rich in the presence of solvent. The boundary conditions of the distribution functions are given by

$$Q_A(-\infty)=1,\ Q_B(-\infty)=Q_C(-\infty)=0$$
$$Q_A(+\infty)=0,\ Q_B(+\infty)=Q_C(+\infty)=1 \quad (19)$$

The surface excess Γ_A in monomers per unit area is usually defined as

$$\Gamma_A/\rho_0=-\int_{-\infty}^{+\infty}dx[\phi_A(x)-\phi_A(-\infty)H(x)] \quad (20)$$

where $H(x)$ is a Heaviside function, $H(x)=1$, for $x\geq 0$ and $H(x)=0$ otherwise. Here the mathematical Gibbs dividing surface, $x=0$, is located at $\Gamma_A=0$.

The expression for the polymer mean field potential, Eq. (12), becomes

$$\omega_P(x)=\Delta\mu_P-\Delta\mu_S \quad (21)$$

where the change of chemical potential can be obtained from the fact that $\Delta f=0$ in the asymptotic phases. The free energy density of the system from Eq. (14) is

$$\Delta f/\rho_0=\sum_K(\mu_{0K}-\mu_K^b)\phi_K(x)+\chi_{AB}\phi_A(x)\phi_B(x)+\chi_{AC}\phi_A(x)\phi_C(x)$$
$$+\chi_{BC}\phi_B(x)\phi_C(x)+\chi_{AS}\phi_A(x)\phi_S(x)+\chi_{BS}\phi_B(x)\phi_S(x)$$
$$+\chi_{CS}\phi_C(x)\phi_S(x)+\phi_S(x)\ln\phi_S(x) \quad (22)$$

The concentration of the small molecule (solvent) adjusts itself at each point to maintain the chemical potential constant.[8] In the two asymptotic phases, the constancy of the solvent chemical potential requires

$$\Delta\mu_S(-\infty)=\Delta\mu_S(+\infty)=0 \quad (23)$$

Using Eq. (22), Eq. (23) gives the following relation between the volume fractions in the two asymptotic phases

$$-\chi_{AS}\phi_A^2(-\infty)-\ln\phi_S(-\infty)-\phi_A(-\infty)=\chi_{BC}\phi_B(\infty)\phi_C(\infty)$$
$$-[\chi_{BS}\phi_B(\infty)+\chi_{CS}\phi_C(\infty)][1-\phi_S(\infty)]-\ln\phi_S(\infty) \quad (24)$$

We also have the following relation:

$$\frac{\phi_A^0}{\phi_A(-\infty)}+\frac{\phi_B^0+\phi_C^0}{\phi_B(\infty)+\phi_C(\infty)}=1 \quad (25)$$

where ϕ_P^0 is the unmixed volume fraction of polymer P. For any choice of ϕ_P^0 and $\phi_B(\infty)$, we can obtain the unknown $\phi_K(\pm\infty)$ by calculating the relations of Eqs. (24) and (25).

Calculation of Physical Properties. Since we assume $Z_P\to\infty$, the third term in Eq. (16) does not contribute to the interfacial tension. We then have

$$\gamma/\rho_0=\int dx\Big\{\Delta f/\rho_0+\sum_P\frac{b^2}{6}\Big[\frac{dq_P(x)}{dx}\Big]^2\Big\} \quad (26)$$

The following equivalent expression[10,11,17] is more convenient.

$$\gamma/\rho_0=2\int dx\Delta f/\rho_0 \quad (27)$$

The excess polymer B (as a compatibilizer) in monomers per unit area, which is the differential adsorption to the interface, is given as like Eq. (20) by

$$\Gamma_B/\rho_0=\int_{-\infty}^{+\infty}dx[\phi_B(x)-\phi_B(\infty)H(x)] \quad (28)$$

As a measure of the thickness of the diffuse interface, we define the widths of the polymers by

$$D_{K=A,C}=\frac{\mp[\phi_K(\pm\infty)-\phi_K(x)]}{[d\phi_K(x)/dx]}\Big|_{\Gamma_K=0} \text{ and } D_B=x|_{\Gamma_C=0} \quad (29)$$
$$D_T=D_A+D_B+D_C$$

where $[d\phi_K(x)/dx]$ denotes the value of the derivative evaluated at the Gibbs dividing surface for polymer A, and at $\Gamma_C=0$ for C. In case of polymer B, $D_B=x|_{\Gamma_C=0}$ is evaluated at $\Gamma_C=0$ relative to the Gibbs dividing surface. In the case of solvent, the width is defined by

$$\Gamma_{BC}/\rho_0=\int_{-\infty}^0 dx[\phi_B(x)+\phi_C(x)]$$
$$+\int_0^{+\infty}dx[\phi_B(x)-\phi_B(\infty)+\phi_C(x)-\phi_C(\infty)]$$
$$D_S=x|_{\Gamma_{BC}=0} \quad (30)$$

where Γ_{BC} is the total amount of polymers B and C adsorbed to the interface, which polymers usually locate in the positive x region from the interface.

The measure of the overlap between the polymers is defined by

$$L_{AK(K=B,C)}=2\int_{-\infty}^{+\infty}dx\phi_A(x)\phi_K(x) \quad (31)$$

Numerical Method

First, for the numerical solutions of Eq. (17) we discretize

the variable x and the mean-field equation by using the generalized Newton's formula[29]

$$\tilde{x}=(i-N)\Delta\tilde{x}, \qquad i=1,\cdots 2N-1 \tag{32}$$

where $\tilde{x}=x/b$ (in reduced unit of length), the equal discrete thickness $\Delta\tilde{x}$ is a constant, and we write $Q_P(x)$ as $Q_P(i)$. In our numerical calculations we used $N=300$ and chose $\Delta\tilde{x}\sim 0.02$. For the calculation of the concentration profiles, two asymptotic values of the distribution function are $Q_P(0)$ and $Q_P(600)$ in Eq. (19).

Equation (17) is rewritten by

$$Q_P(i)''=6\omega_P(i)Q_P(i) \tag{33}$$

The discretized mean-field equation has the following form in i.

$$\Delta Q_P(i)=\frac{\lambda(\Delta\tilde{x})^2}{2}\left\{\frac{[Q_P(i+1)-2Q_P(i)+Q_P(i-1)]/(\Delta\tilde{x})^2-F(Q_P)}{1+\frac{(\Delta\tilde{x})^2}{2}\frac{\partial F(Q_P)}{\partial Q_P(i)}}\right\} \tag{34}$$

where λ is some relaxation parameter (here, we chose $\lambda\sim 0.5$), $F(Q_P)=Q_P''$, and $\Delta Q_P(i)=Q_P^{new}(i)-Q_P^{old}(i)$.

We begin with the guess for $Q_P(i)$ which is chosen as a trial distribution function, $Q_P(i)\sim[1+\tanh\{(6\chi_{AB})^{0.5}i\}]^{0.5}$, and we then calculate $\phi_P(i)$ by using Eq. (18). By using Eqs. (24) and (25), we obtain the volume fractions, $\phi_K(\pm\infty)$, in the asymptotic phases. We use Eqs. (21), (22), and $\phi_K(\pm\infty)$ to obtain the initial guess for $\omega_P(i)$. We then solve the discretize mean-field equation, Eq. (34) with the help of the boundary conditions, Eq. (19). We thus obtain the set of $\Delta Q_P(i)$ and $\Delta Q_P^{new}(i)$, Here we refer $\Delta Q_P^{new}(i)$ to $\Delta Q_P^{old}(i)$.

From the set of $\Delta Q_P^{new}(i)$, we get the new concentration profile $\phi_P^{new}(i)$ by using Eq. (18). The new mean field, $\omega_P^{new}(i)$, is calculated by using $\phi_P^{new}(i)$, Eq. (21), and Eq. (22) again. By this we obtain the set of $\Delta Q_P(i)$ and $Q_P^{new}(i)$ again and refer $Q_P^{new}(i)$ to $Q_P^{old}(i)$.

This iteration process is continued until the following condition is satisfied

$$\max_{i=1,\cdots,2N-1}|\Delta Q(i)=Q_P^{new}(i)-Q_P^{old}(i)|\leq\varepsilon(\sim 10^{-6}) \tag{35}$$

After convergence, we obtain $Q_P(i)$ and finally obtain $\phi_P(i)$ using Eq. (18). Then a solvent concentration profile can be obtained by

$$\phi_S(i)=1-\sum_P\phi_P(i) \tag{36}$$

Results and Discussion

Four parameters used in this polymers/solvent system are as follows: χ_{AC}, χ_{BC} (as negative value), the volume fraction of B in the asymptotic phase, $\phi_B(\infty)$, and that of solvent, ϕ_S^0. In this blends the relation between the unmixed volume fractions for the polymers is always $\phi_B{}^0=\phi_C{}^0=\phi_A{}^0/2$, and the polymer-solvent interaction parameters are fixed as follows: $\chi_{AS}=1.0$, $\chi_{BC}=0.8$, and $\chi_{CS}=0.8$, χ_{AB} is also fixed as $\chi_{AB}=0.5$. We, first, selected the reference system with a particular set of parameters that will serve as a basis: $\chi_{AC}=1.5$, $\chi_{BC}=-0.2$, $\phi_S{}^0=0.2$, and $\phi_B(\infty)=0.4$.

Figure 1 shows the concentration profiles of polymers (A, B, and C) and solvent (S) as the reference. The repulsive interaction between A and C usually drives C away from the interface, and B then easily is located in the interfacial region. When the attractive interaction between B and C is small, in the same way, the polymers A and B mainly remain near the interface. In Figure 1 we can see the strong adsorption of B to the interface in spite of the same quantities of B and C in the asymptotic mixture phase, and also the adsorption of solvent. Figure 2, with the same conditions as in Figure 1, shows that the value of ϕ_S increases with increasing $\phi_S{}^0$. A solvent competes with the polymer B (as a compatibilizer) in the interfacial region, but it is preferentially adsorbed to the interface. This trend also leads to the

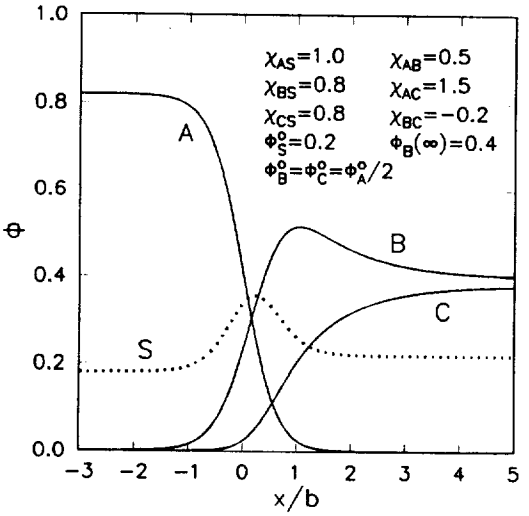

Figure 1. Concentration profiles of polymers (A, B, and C) and solvent (S) as a reference. The relation between the unmixed volume fractions for the polymers is always $\phi_B{}^0=\phi_C{}^0=\phi_A{}^0/2$, and the Flory interaction parameters are as follows: $\chi_{AS}=1.0$, $\chi_{BS}=0.8$, $\chi_{CS}=0.8$, $\chi_{AB}=0.5$, and $\chi_{BC}=-0.2$. The same parameters are used in all the figures hereafter. This figure also has three variables: $\chi_{AC}=1.5$, $\phi_S{}^0=0.2$, and $\phi_B(\infty)=0.4$. The plane, $x/b=0$ shows the Gibbs dividing surface for polymer A.

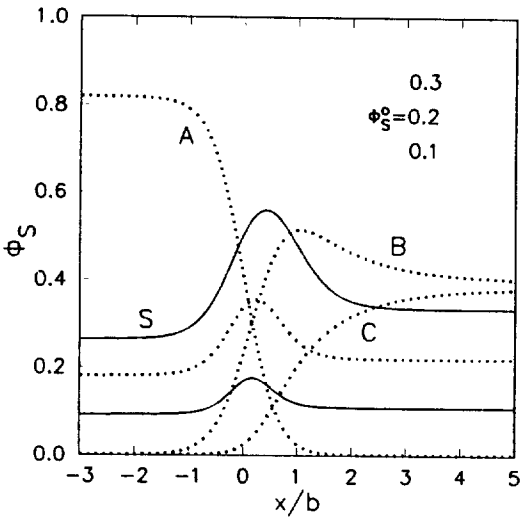

Figure 2. Interfacial concentration profiles of solvent (S) for varying $\phi_S{}^0$ with $\chi_{AC}=1.5$ and $\phi_B(\infty)=0.4$. The dotted lines indicate the same reference as in Figure 1.

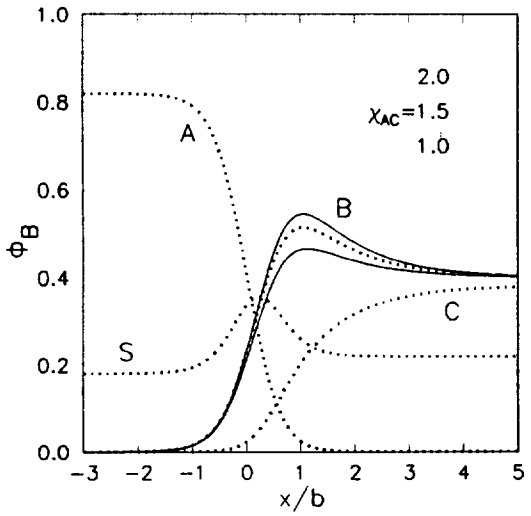

Figure 3. Interfacial concentration profiles of polymer (B) for varying χ_{AC} with $\phi_S^0=0.2$ and $\phi_B(\infty)=0.4$. The dotted lines indicate the same reference as in Figure 1.

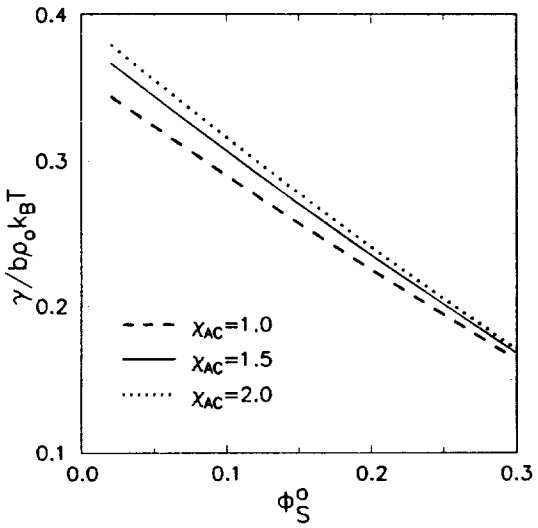

Figure 4. Variation of the interfacial tension, in units of $b\rho_0k_BT$, with ϕ_S^0 for varying χ_{AC} with the same conditions as in Figure 3. The solid lines in Figures 4-7 indicate a reference corresponding to $\chi_{AC}=1.5$, $\phi_S^0=0.2$, and $\phi_B(\infty)=0.4$.

reduction of the interfacial tension.

Effect of Varying ϕ_S^0 for Different χ_{AC}. Figures 3-7 show how the repulsive interaction between polymers A and C can modify the interfacial properties. In Figure 3 we can see the increasing adsorption of polymer B with χ_{AC} because of the repulsive interaction between A and C. As χ_{AC} approaches to χ_{AB}, the polymer A gradually feels the similar degree of the interaction against B and C, and therefore the concentration profiles of B and C nearly remain constant. In Figure 4 as ϕ_S^0 increases, in given some χ_{AC} the interfacial tension reduces as we expected in Figure 2, and as increasing χ_{AC}, C is driven away from the overlap with A in the interfacial region, so the resulting some high interfacial tension. In Figure 5 the excess polymer B decrease with ϕ_S^0 because of the preferential adsorption of solvent to the interface. The

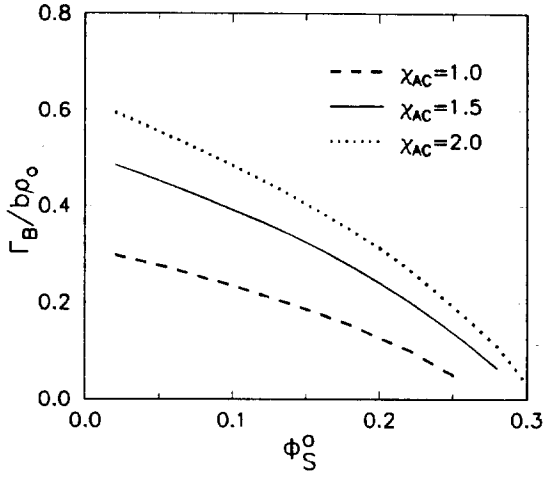

Figure 5. Variation of the excess polymer B per unit area, in units of $b\rho_0$, with ϕ_S^0 for varying χ_{AC}.

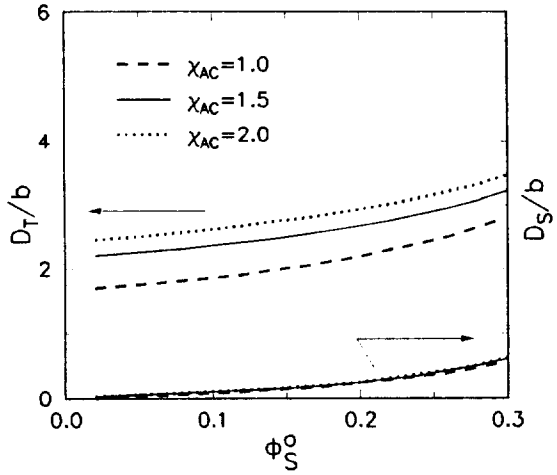

Figure 6. Variation of the widths of the interface and solvent, in units of b, with ϕ_S^0 for varying χ_{AC}.

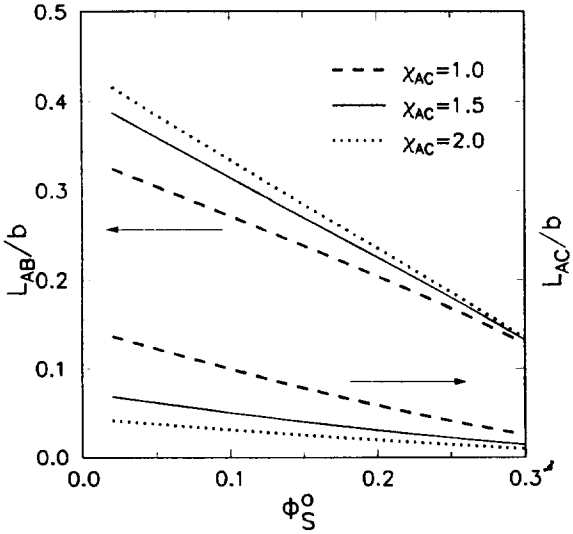

Figure 7. Variation of the overlap lengths between polymers, in units of b, with ϕ_S^0 for varying χ_{AC}.

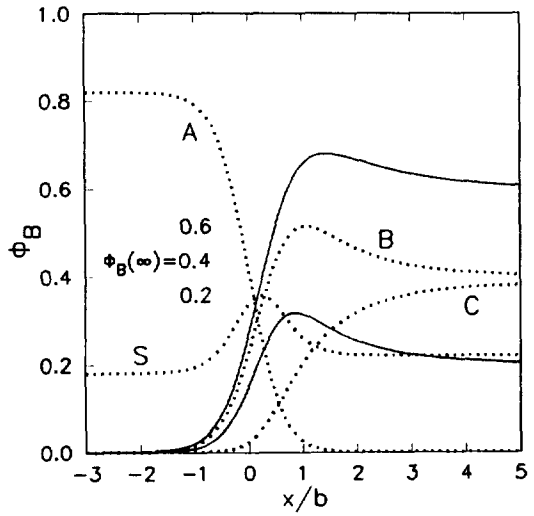

Figure 8. Interfacial concentration profiles of polymer *B* for varying $\phi_B(\infty)$ with $\chi_{AC}=1.5$ and $\phi_S^0=0.2$. The dotted lines indicate the same reference as in Figure 1.

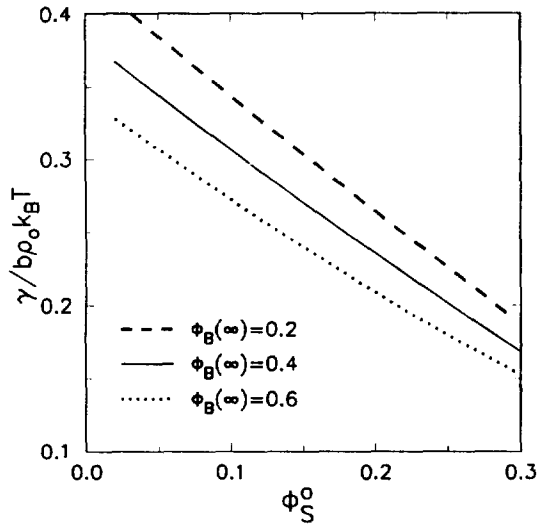

Figure 9. Variation of the interfacial tension, in units of $b\rho_0 k_BT$, with ϕ_S^0 for varying $\phi_B(\infty)$ with the same conditions as in Figure 8. The solid lines in Figures 9-12 indicate the same reference as in Figure 4.

widths of the interface and solvent increase as increasing ϕ_S^0, but the interfacial width is mainly affected by the adsorption of solvent in the constant amount of polymer *B*, as shown in Figure 6. Figure 7 shows the measure of overlap between the polymers against ϕ_S^0. As ϕ_S^0 increases, the polymers *B* and *C* are driven away from the interface where *A* is present. When χ_{AC} is small, the overlap length between *A* and *C* becomes short, and in Figure 6 the interfacial width also becomes narrow. χ_{BC} is the measure of the attractive interaction between *B* and *C*, *i.e.*, increasing of χ_{BC} as negative value has the opposite effect to χ_{AC} for the interfacial tension, the excess polymer *B*, the interfacial width, and the overlap lengths between the polymers.

Effect of Varying ϕ_S^0 for Different $\phi_B(\infty)$. In this part Figures 8-12 show how the quantity of compatibilizer, $\phi_B(\infty)$,

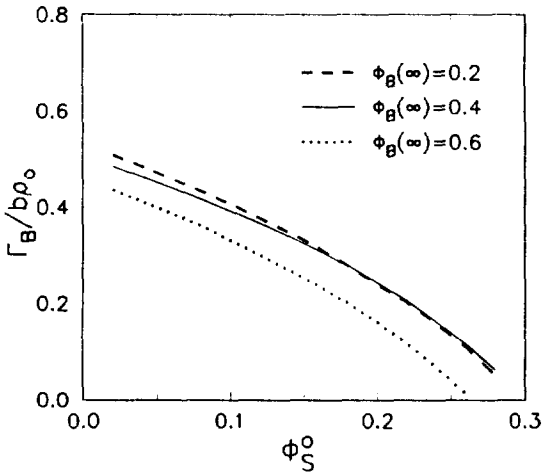

Figure 10. Variation of the excess polymer *B* per unit area, in units of $b\rho_0$, with ϕ_S^0 for varying $\phi_B(\infty)$.

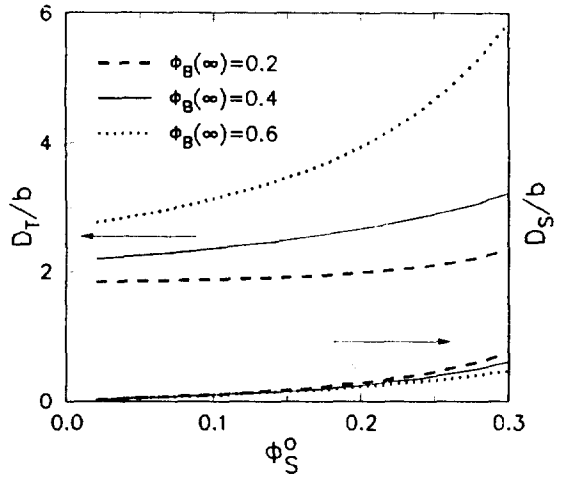

Figure 11. Variation of the widths of the interface and solvent, in units of *b*, with ϕ_S^0 for varying $\phi_B(\infty)$.

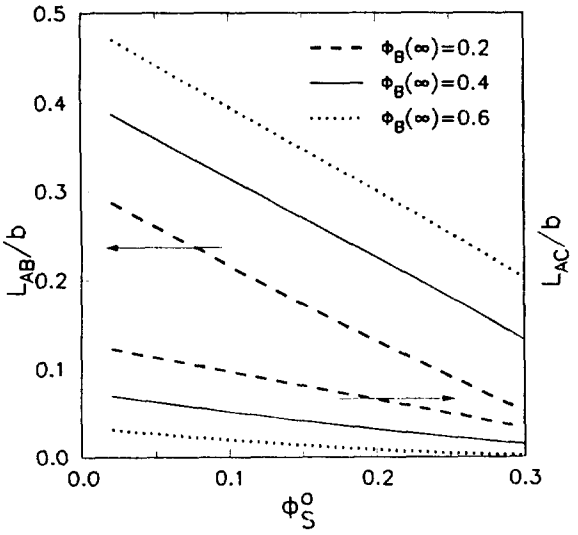

Figure 12. Variation of the overlap lengths between polymers, in units of *b*, with ϕ_S^0 for varying $\phi_B(\infty)$.

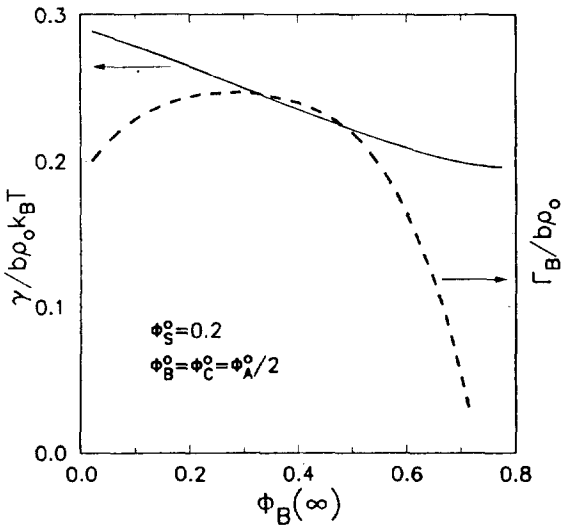

Figure 13. The interfacial tension, in units of $b\rho_o k_B T$, and the excess polymer B per unit area, in units of $b\rho_o$, are plotted against $\phi_B(\infty)$ with $\phi_S^0=0.2$ and $\chi_{AC}=1.5$.

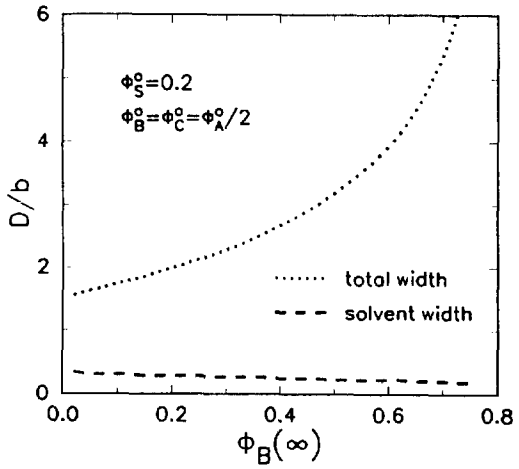

Figure 14. Total width of interface (dotted line) and solvent (dashed line), in units of b, are plotted against $\phi_B(\infty)$ with the same conditions as in Figure 13.

can modify the interfacial properties as increasing of the solvent concentration. Figure 8 shows the concentration profiles of B for different values of $\phi_B(\infty)$. We can see that even if the amount of B in the asymptotic mixture phase is small, it can lead to a considerable adsorption to the interface. In large $\phi_B(\infty)$ the concentration profile of B becomes flat and the interface thick, but the excess B decreases on the contrary. In Figure 9 the interfacial tension for some $\phi_B(\infty)$ rapidly decreases with ϕ_S^0. It can lead to the improvement of the interfacial adhesion between polymers A and C, and thus slow the phase demixing process of the blends. The reduction of the interfacial tension against ϕ_S^0 ranging from 0.1 to 0.3 is expressed by $\gamma \propto [\phi_S^0]^{-0.6}$, as shown in Figures 4 and 9. Figure 10 shows the dependence of the excess B on the solvent volume fraction. In high concentration, $\phi_B(\infty)=0.6$, there is a small amount of B adsorbed to the interface, as we expect in Figure 8. We will discuss more about the behavior at small and large $\phi_B(\infty)$ below. Figure 11 shows the widths of the interface and solvent. The broadening effect of the interface is mainly affected by the adsorption of solvent in a small amount of polymer B. When $\phi_B(\infty)$ is high, the width of the interface considerably becomes thick with ϕ_S^0. Figure 12 shows the overlap lengths between the polymers with ϕ_S^0. In high ϕ_S^0 we can see that the strong dependence of L_{AB} occurs in the variation of $\phi_B(\infty)$, but not in χ_{AC}, as shown in Figures 7 and 12.

Effect of Varying $\phi_B(\infty)$. Figure 13 shows the dependence of the interfacial tension and the excess polymer B on the volume fraction, $\phi_B(\infty)$, with $\phi_S^0=0.2$. From the solid line, the reduction of the interfacial tension against $\phi_B(\infty) \geq 0.2$ can be expressed by $\gamma \propto [\phi_B(\infty)]^{-0.25}$. This shows that the strong dependence of the interfacial tension occurs in the variation of ϕ_S^0 when we compare Figures 4 and 9 with Figure 13. The dotted curve, the excess B, shows the similar tendency to the model without a solvent. The maximum point appears in the medium region, and in small and large $\phi_B(\infty)$ the excess B decreases. This result is due to the fact that the amount of B adsorbed to the interface is estimated by the amount of B in the interfacial region and the relative one for B in the asymptotic mixture phase, as expressed in Eq. (28). Figure 14 shows that the width of solvent in the constant amount of solvent is not nearly affected by the amount of B, and the interfacial width only increases with $\phi_B(\infty)$. It also shows the polymer B competes with solvent in the interfacial region.

Concluding Remarks

In this paper we present the results of a theoretical study of the interfacial properties of the polymer/polymer mixture system including a solvent. By solving the mean-field equations numerically in the limit of infinitely large molecular weight for the polymers and a vanishingly small compressibility, we obtained the concentration profiles of polymers (A, B, and C) and solvent (S), the interfacial tension, the amount of polymer B adsorbed to the interface, the widths of total interface and solvent, and the overlap lengths between the polymers for various typical values of two Flory interaction parameter, χ_{AC} and χ_{BC}, the volume fraction of B in the asymptotic mixture phase, $\phi_B(\infty)$, and the unmixed one of solvent, ϕ_S^0.

A solvent competes with the polymer B (as a compatibilizer) in the interfacial region, but it is preferentially adsorbed to the interface. This shows the strong dependence of the interfacial tension on ϕ_S^0 as $\gamma \propto [\phi_S^0]^{-0.6}[\phi_B(\infty)]^{-0.25}$ within ϕ_S^0 ranging from 0.1 to 0.3 and $\phi_B(\infty)$ above 0.2.

Even a small amout of polymer B in the asymptotic mixture phase can modify the interfacial properties. As increasing $\phi_B(\infty)$, the interfacial tension decreases, the width of the interface and the overlap length between A and B increase, and the excess polymer B also increases as like the A/BC system[6] without a solvent, which is a considerable amount in very small $\phi_B(\infty)$ and slowly decreases in large $\phi_B(\infty)$ above around 0.4.

Increasing χ_{AC} repels the polymer C from the interfacial region, consequently it leads to an increasing adsorption of polymer B, the overlap length between A and B, the interfacial width, and the interfacial tension. Increasing $|\chi_{BC}|$ has

the opposite effect to χ_{AC} except the interfacial tension among the interfacial properties, even if not shown in this paper.

Acknowledgment. The present study was supported (in part) by the Basic Science Research Institute Program, Ministry of Eduction, Korea, 1993. Project No. BSRI-93-309.

References

1. Kryszewski, M.; Galeski, A.; Martuscelli, E. *Polymer Blends*; Proceeding of the Second Italian-Polish Joint Seminar on Multicomponent Polymeric Systems; held 1982; Plenum Press: New York, 1984; Vol. 2.
2. Han, C. D. *Polymer Blends and Composites in Multiphases Systems*; *ACS*, **1984**, 206.
3. Anastasiadis, S. H.; Gancarz, I.; Koberstein, J. T. (a) *Macromolecules* **1988**, *21*, 2980; (b) *ibid.* **1989**, *22*, 1449.
4. Shull, K. R.; Kellock, A. J.; Deline, V. R.; MacDonald, S. A. *J. Chem. Phys.* **1992**, *97*, 2095.
5. Budkowski, A.; Steiner, U.; Klein, J. *J. Chem. Phys.* **1992**, *97*, 5229.
6. Yoon, K.-S.; Pak, H. *Bull. Korea Chem. Soc.* **1994**, *15*, 45.
7. Helfand, E. *J. Chem. Phys.* **1975**, *63*, 2192; Roe, R.-J. *ibid.* **1975**, *62*, 490.
8. (a) Helfand, E.; Tagami, Y. *J. Chem. Phys.* **1972**, *56*, 3592; (b) *ibid.* **1972**, *57*, 1812.
9. Helfand, E. *J. Chem. Phys.* **1975**, *62*, 999.
10. Helfand, E.; Sapse, A. M. *J. Chem. Phys.* **1975**, *62*, 1327.
11. Hong, K. M.; Nooland, J. *Macromolecules* **1980**, *13*, 964.
12. Hong, K. M.; Nooland, J. *Macromolecules* **1981**, *14*, 736.
13. Hong, K. M.; Nooland, J. *Macromolecules* **1981**, *14*, 727.
14. Nooland, J.; Hong, K. M. (a) *Macromolecules* **1982**, *15*, 482; (b) *ibid.* **1984**, *17*, 1531.
15. Whitmore, M. D.; Nooland, J. *J. Chem. Phys.* **1990**, *93*, 2946.
16. Vilgis, T. A.; Nooland, J. *Macromolecules* **1990**, *23*, 2941.
17. Helfand, E. *Macromolecules* **1992**, *25*, 1676.
18. Tagami, Y. *J. Chem. Phys.* **1980**, *73*, 5354; de la Cruz, M. O.; Edward, S. F.; Sanchez, I. C. *ibid.* **1988**, *89*, 1704; Hong, K. M.; Nooland, J. *Macromolecules* **1981**, *14*, 1229.
19. (a) Helfand, E.; Bhattacharjee, S. M.; Fredrickson, G. H. *J. Chem. Phys.* **1989**, *91*, 7200; (b) Broseta, D.; Fredrickson, G. H.; Helfand, E.; Leibler, L. *Macromolecules* **1990**, *23*, 132.
20. Koberstein, J. T., in *Encyclopedia of Polymer Science and Engineering*; ed. by Mark, H. F.; Bikales, N. M.; Overberger, C. G.; Menges, G.; Kroschwitz, J. I. Wiley-Interscience: 1987; Vol. 8.
21. Wang, S.; Shi, Q. *Macromolecules* **1993**, *26*, 1091.
22. (a) Rowlinson, J. S.; Widom, B. Chap. 3 of *Molecular Theory of Capillarity*; Oxford University Press: New York, 1982; (b) Cahn, J. W.; Hilliard, J. E. *J. Chem. Phys.* **1958**, *28*, 258.
23. Edward, S. F. *Proc. Phys. Soc.* **1965**, *85*, 613.
24. Freed, K. F. *Adv. Chem. Phys.* **1972**, *22*, 1.
25. Weigel, F. W. *Introduction to Path-Integral Methods in Physics and Polymer Science*; World Scientific 1986.
26. Adamson, A. W. Chap. III of *Physical Chemistry of Surfaces*; 5th ed.; Wiley-Interscience: 1990.
27. Flory, P. J. *Principles of Polymer Chemistry*; Cornell University Press: Ithaca, New York, 1953.
28. de Gennes, P. G. *Scaling Concepts in Polymer Physics*; Cornell University Press: Ithaca, New York, 1979.
29. Greenspan, D. Chap. 1 of *Discrete Numerical Methods in Physics and Engineering, Mathematics in Science and Engineering Series*; Academic Press: 1974; Vol. 107.

Structures and Barrier Heights for the Internal Rotation of Ethyl Halides Caculated by *ab initio* Methods

Ungsik Ryu and Yoon Sup Lee

Department of Chemistry and Center for Molecular Science, Korea Advanced Institute of Science and Technology, Taejon, 305-701

Received October 13, 1993

The barrier heights of the internal rotations for ethyl halides calculated by *ab initio* methods differ from those of experiments by more than 0.2 kcal/mol. The use of basis sets larger than the 6-31G* set and the inclusion of correlation do not improve the agreement between the calculated and experimental values. The zero-point vibration corrections are substantial in the HF calculations with 6-31G* basis sets, but become negligible in the MP2 calculations with 6-311G** basis sets for C_2H_5F and C_2H_5Cl. It is shown that the rigid rotor approximation and the assumed shape of the potential curve as a cos2θ curve could also be the sources of discrepancies between calculated and experimental values. Higher order perturbation corrections narrow the gap between experimental and theoretical values, but there still remains about 10% overestimate of 0.3 kcal/mol. Optimized geometries from the HF and MP2 calculations are in good agreement with those from experiments. Dipole moments calculated from the MP2 densities show slightly better agreement with experiments than those from the HF densities.

Introduction

Ethyl halides are one of the simplest systems that exhibit internal rotations. Barrier heights of internal rotations for ethyl halides (C_2H_5X where X=F, Cl, Br and I) do not display any apparent trends as the halogen atom varies from